

Pattern differentiation of glandular cancerous cells and normal cells with cellular automata and evolutionary learning

Jong-Chen Chen ^{a,*}, Chun-Ming Yeh ^a, Jeh-En Tzeng ^b

^a Department of Information Management, National YunLin University of Science and Technology, Touliu, Taiwan, ROC

^b Department of Pathology, Buddhist Dalin Tzu Chi General Hospital, Chiayi, Taiwan, ROC

Abstract

The examination of morphological features is used as a universal procedure by pathologists to determine whether cells are cancerous. Generally speaking, the shapes of normal cells are more standard (either circular or oval) than those of cancerous cells. The objective of this study was to construct an autonomous feature detection system, with the hope of finding some feature patterns, based on morphological shapes (contours), that could be used to separate cancerous cells from normal cells. A number of feature detectors (FDs) were initially generated at random. Then they were modified through evolutionary learning and cellular automata. The experimental result showed that this system was able to search appropriate FDs to identify cancerous cells in a self-organizing manner. It also showed that these FDs were general so that each of them could be used to identify more than one cancerous cell, and that there existed some common patterns of cell deformity among cancerous cells. This system was also applied to two other domains, and achieved satisfactory experimental results.

© 2006 Elsevier Ltd. All rights reserved.

Keywords: Cellular automata; Evolutionary learning; Pattern recognition

1. Introduction

The smear test, a cytological diagnostic method, was initiated a century ago and is still one of the common diagnostic tools that pathologists use to detect malignant cells. It is conducted by removing a small quantity of tissue or body fluid from living body, which is then thinly spread on a slide for microscopic image analysis. Generally speaking, the contours of normal and benign cells are typically uniform (or smooth). More specifically, they are either circular or oval. In contrast, the shapes of malignant cells are more irregular than those of normal and benign cells. This is because cancerous cells are active due to the reproductive and mitotic behaviors occurring inside the nucleus, which might cause anisonucleosis (uneven or unequal nuclei), nuclear enlargement, multi-nuclei, nuclear deformity (or

cytoplasmic deformity), various cell sizes, large nucleocytoplasmic ratio, irregular chromatin distribution, and proliferation of malignant cells.

However, it is not necessarily true that all cancerous cells do possess all of these noticeable cellular changes. And a cell with any of these changes does not absolutely indicate that it is cancerous. The task is thus difficult because there is not a single mechanism that can be used to distinguish between normal and cancerous cells unambiguously. As a consequence, it is strictly dependent on personal experience. However, human error is sometimes inevitable. Image analysis using autonomous, computer-based methods is getting more important as it may provide a second opinion to pathologists.

The studies of applying computer on microscopic cell image analysis can be roughly divided into three stages: contour identification (including segmentation), feature extraction, and classification. The first stage is to find out the boundary (contour) of a cell and its nucleus, including noise removal and image enhancement (Thiran & Macq,

* Corresponding author. Tel.: +886 5 534 2601x5300 (Dept.), +886 5 534 2601x5332 (Office), +886 5 551 2762 (Home); fax: +886 5 531 2077.
E-mail address: jcchen@mis.yuntech.edu.tw (J.-C. Chen).

1996; Leung, Chan, Lam, Kwok, & Chen, 2000; Schnorrenberg, Pattichis, Kyriacou, & Schizas, 1997; Schnorrenberg et al., 2000). However, in some cases, cells tend to be clustered together so that it is not easy to separate them on a two-dimensional image. An extra effort must be made on image segmentation and shape discrimination (e.g. Anoraganingrum, 1999; Wang, Zeng, Yu, Wang, & Xia, 2001; Wu, Barba, & Gil, 1996).

Feature extraction is the next stage after cell identification. As there are several prominent features that can be extracted from a cell, a number of studies on feature extraction have been carried out (Bisconte & Margules, 1980; Travo, Bodin, Burnstock, & Stoclet, 1987), shape (Thiran & Macq, 1996), color hue (Garbay, Chassery, & Brugal, 1986; Gauvain, Seigneurin, & Brugal, 1987), gray-scale and gradient (Chen, Xie, Zhang, & Xia, 2001), and texture (Hu et al., 1994; Liu, Zhao, & Zhang, 2002; Schnorrenberg et al., 1997).

The last stage is to differentiate between cancerous cells and normal cells. Artificial neural network approaches are used by several investigators (Chen et al., 2001; Hu et al., 1994; Kim, 1999; Moallemi, 1991; Naguib et al., 1999; Wang et al., 2001). In these models, they directly apply the features (or parameters) obtained in the previous stage to perform cell classification. We note that some of these models, to some extent, do demonstrate satisfactory results in differentiating these two types of cells. However, little information is provided about what specific patterns of cell deformity are more tentative for cells to be cancerous than being normal. And there are very few models that combine feature extraction and cell differentiation into a system. Thiran & Macq (1996) propose a model that includes both feature extraction and cell differentiation. They organize a set of rules in order to help extract the features that most pathologists use to decide whether the tissue is cancerous or not. The features extracted include nucleocytoplasmic ratio, anisonucleosis, nuclear deformity, and hyperchromasia. Then, they apply a grading rule that takes these four features into account so as to make a diagnosis. However, strictly speaking, this dedicated system is rigid in a sense that the mechanisms of feature extractions, including its cell differentiation rules, are set up in a predetermined manner.

The objective of this study was to find some feature detectors (FDs) that could be used to separate between cancerous cells and normal cells, and to investigate what patterns of cell deformity were more likely to be cancerous. The ultimate goal was that we could use each of these FDs to identify a number of cancerous cells, instead of just one cell. The existence of such FDs implied that there existed some common patterns among cancerous cells. From these patterns, people might gain an insight into the commonality of cancerous cells. Moreover, it might provide valuable information for those people who were interested in the formation and development of cancerous tissue.

It was absolutely not an easy job to find such FDs. Let us take an 8×8 grid of binary feature detectors as an exam-

ple. The number of possible FDs was substantially large (i.e., 2^{64}). Indeed, it grew combinatorial with the size of a feature detector. The goal of this study was to construct a system that could generate and modify FDs for specific pattern recognition domains in a self-organizing manner. The evolutionary learning algorithm was used (Bremermann, 1962; Rechenberg, 1973; Conrad, 1974; Fogel, 1995; Fogel, Owens, & Walsh, 1966). The Darwinian variation–selection mechanism had two major operators: variation and selection. In this study, we used the variation operator to explore the FD repertoire on the one hand and the selection operator to confine the search space on the other. Cellular automata (CA) proposed by Ulam and von Neumann in 1950 was used to vary FDs. The details will be described in Section 2. The application domains and the experimental results are presented in Section 3. Finally, Section 4 provides discussion and conclusions.

2. Materials and methods

In this section, we first explained how to obtain the contour of each cell from the microscopic images of cytological specimens. Then, we illustrated how to determine the similarity between an FD and a cell pattern. Finally, we showed the evolutionary learning algorithm that we used in this model, including the cellular automata rules.

2.1. Image pre-processing

Our experimental data include the microscopic cell images of pleural effusion. They were taken from one of the major hospitals in Taiwan. To obtain such an image, pathologists took a small amount of pleural effusion from a patient and concentrated the cells on a glass surface by cytospin. The next step was to dye the cells. Finally, a digital camera was used to digitize the images of dyed cells.

Fig. 1 shows two of these microscopic images that we used in this study. For each of these microscopic images, our first step was to identify the contour of each cell. In the present study, only isolated cells were considered (i.e., we ignored the aggregated cells). We used *Photo Impact* (version 7.0), an image editing tool, to remove noises, to get rid of undesired components, and to find the contour of each cell. Fig. 2 shows some of these cancerous cells and normal cells. Note that these *Photo Impact* files were saved in the bit mapped format. These files were then converted into ASCII format using *ASCII Pic* (an application system for transforming a file in bit mapped format into ASCII format). Fig. 3 shows an example of a cell image in ASCII format, consisting of 32×32 bits. Lastly, we wrote a small program to find the contour of each cell (Fig. 4).

Note that at the present time we use a number of commercial tools to pre-process the microscopic images, instead of developing our own system. The pre-processing work includes the removal of noises and undesired compo-

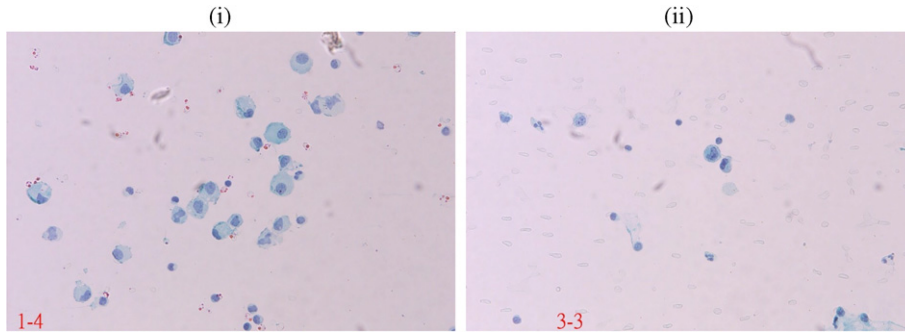


Fig. 1. Microscopic cell images. (i) Normal cells and (ii) cancerous cells.

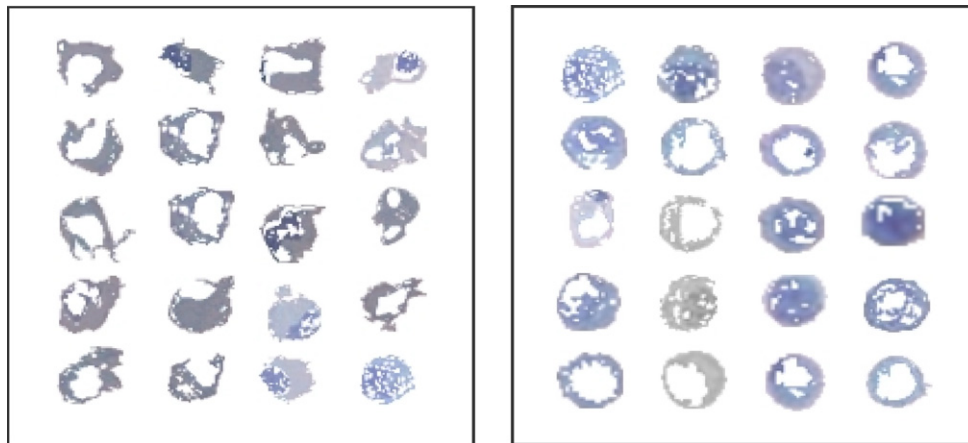


Fig. 2. Cancerous cells (left) and normal cells (right).

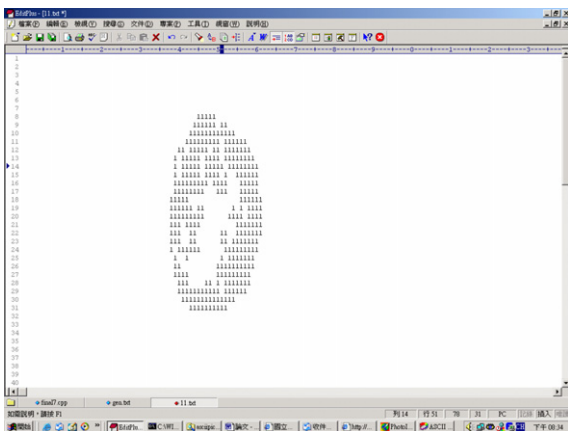


Fig. 3. A cell in ASCII format.

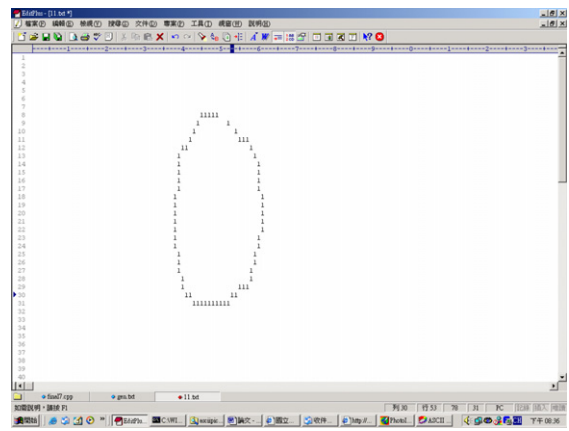


Fig. 4. A cell contour.

nents and the segmentation of overlapped cells. Our interest in this study was to develop a system that could find feature detectors in a self-organizing manner (through evolutionary learning) for assisting pathologists in correctly separating cancerous cells from normal cells. Eliminating the image pre-processing work allowed us to put the emphasis on feature detection and pattern recognition.

2.2. Pattern matching

In this system, FDs served as an arbiter that would be used to separate cancerous cells from normal cells. A cell was diagnosed as cancerous if part of its pattern matched any one of the FDs in this system. On the contrary, a cell was diagnosed as normal if none of the FDs matched it.

We assumed that the size of an FD was comparatively smaller than that of a cell pattern. As there was no preliminary information regarding which part of a cell might match an FD, we had to search every possible portion of a cell pattern. It was implemented by decomposing a cell pattern into a number of sub-patterns, based on the size of the FD. We compared every FD with each of these sub-patterns to determine their similarity. For example, a pattern with a size of 32×32 bits would be decomposed into 625 sub-patterns (i.e., $((32 - 8) + 1) * ((32 - 8) + 1)$)

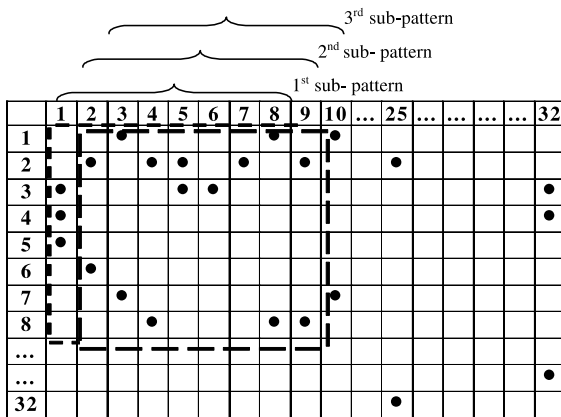


Fig. 5. Decomposition of a cell pattern.

if an FD with a size of 8×8 bits was used (Fig. 5). We noted that it was possible that an FD might match a sub-pattern in other orientations. Thereby, we also tested the similarity of a sub-pattern with an FD rotated at 90° , 180° , and 270° , respectively. The fitness on its best fit sub-pattern was assigned as the fitness of an FD on a cell pattern.

The next step was to measure the similarity between a sub-pattern and an FD. The performance parameter we used was the minimum square of difference (MSD). Each sub-pattern, including each FD, was encoded with two pairs of vectors: horizontal and vertical. The similarity between an FD and a sub-pattern was determined by the sum of the MSDs on their horizontal and vertical pairs of vectors. The lower the sum of MSDs, the higher the similarity was.

The following explained how to encode the horizontal pair of vectors. First, we horizontally divided a pattern into two halves: top and bottom. For each half, we numbered each row in sequence from the inner-most (the one closest to the center line) to the outer-most row (Fig. 6). Two vectors were used, one for each half. The first element of a vector encoded the bit information of the first column, the second number the second column, and so on. The value assigned to each element was the row number of the

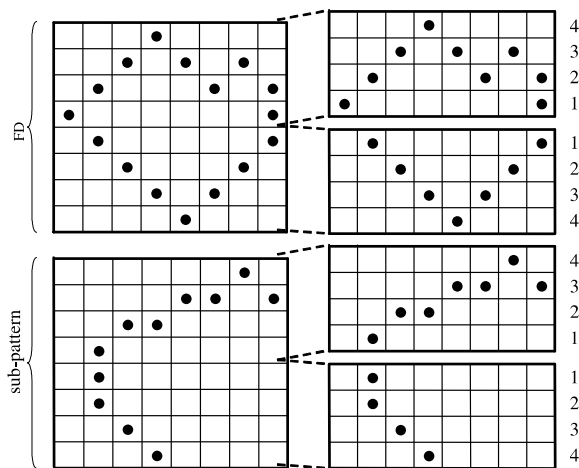


Fig. 6. Horizontally divide an FD and a sub-pattern.

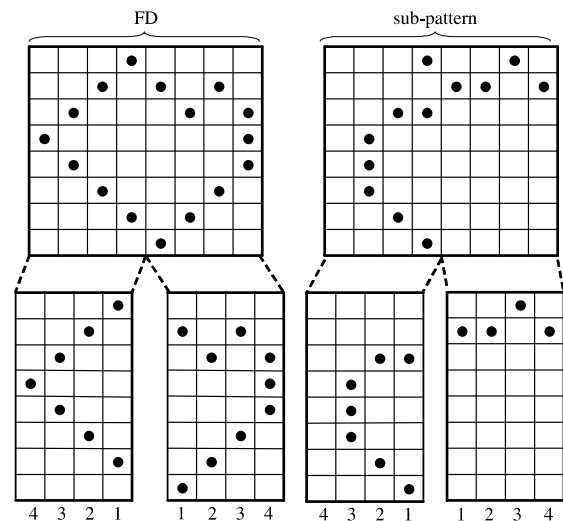


Fig. 7. Vertically divide an FD and a sub-pattern.

Table 1
Encoded vectors for Fig. 6

FD (top)	1	2	3	4	3	2	3	2
FD (bottom)	0	1	2	3	4	3	2	1
Sub-pattern (top)	0	1	2	2	3	3	4	3
Sub-pattern (bottom)	0	2	3	4	0	0	0	0

$$MSD_{top} = (1 - 0)^2 + (2 - 1)^2 + (3 - 2)^2 + (4 - 2)^2 + (3 - 3)^2 + (2 - 3)^2 + (3 - 4)^2 + (2 - 3)^2$$

$$MSD_{bottom} = (0 - 0)^2 + (1 - 2)^2 + (2 - 3)^2 + (3 - 4)^2 + (4 - 0)^2 + (3 - 0)^2 + (2 - 0)^2 + (1 - 0)^2$$

outer-most bit in its corresponding column. The vectors encoded for Fig. 6 are shown in Table 1. Fig. 7 shows how to vertically divide a pattern into two halves: left and right. The encoding mechanism of the vertical pair of vectors was similar to that of the horizontal pair.

2.3. Evolutionary algorithm

To separate cancerous cells from normal cells, we placed three hypotheses. The first was possible to identify (detect) a cancerous cell from its partial pattern. In other words, to decide whether a cell was cancerous or not, it was not necessary to examine an entire pattern. Without this hypothesis, it would not be possible to find FDs that could be used to separate cancerous cells from normal cells. This was why we assumed that the size of an FD was comparatively smaller than that of a cell pattern. The second hypothesis was that we could separate these two types of cells by their contours (not including cell size, nucleus contour, nucleocytoplasmic ratio, chromatin distribution, etc.). The third hypothesis was that there existed some common patterns among cancerous cells. This was important as we hoped to find general FDs that each of them could be used to identify a number of cancerous cells, not just one.

The fitness of an FD was determined by how well we could use it to separate cancerous cells from normal cells. Note that a good FD was defined as it had a good match with at least one of the cancerous cells but did not match any of the normal cells. FDs were generated at random in the beginning and modified through evolutionary learning. The algorithm is shown in Fig. 8. After evaluating the fitness of each FD, we copied them with the variation from best-performing to lesser-performing. Cellular automata (CA) were used to modify (vary) the lesser-performing FDs. That is, the change of an FD was based on a specific cellular automata rule.

The following explained how to use CA to evolve FDs. Cellular automaton consisted of a lattice of sites. Each site had a number of states. The state of each site was updated in discrete time steps, depending on its present state and the states of its neighboring sites. Each FD was represented with a two-dimensional grid of bits. To vary FDs, we used two-dimensional cellular automata. There were several possible lattices and neighborhood structures for two-dimensional cellular automata. In the present implementa-

1. **Generate** a group of feature detectors *FDs* at random.
2. **Evaluate** the fitness of each *FD*.
3. **Select** three best-performing *FDs* for reproduction.
4. **Copy** the best-performing *FDs* to the lesser-performing *FDs*.
5. **Mutate** the lesser-performing *FDs*. It was implemented by randomly choosing some pixels and then applying each of these with a specific cellular automata rule.
6. **Go to Step 2** unless the stopping criteria are satisfied.

Fig. 8. Evolutionary learning of FDs.

Table 2
Cellular automata rules

Rule number	$[S_{i-1,j}S_{i+1,j}S_{i,j-1}S_{i,j+1}S_{i,j}]$ at time t				
	[11111]	[...]	[00010]	[00001]	[00000]
1	0	...	0	0	0
2	0	...	0	0	1
3	0	...	0	1	0
4	0	...	0	1	1
5	0	...	1	0	0
6	0	...	1	0	1
7	0	...	1	1	0
8	0	...	1	1	1
...
4,294,967,296	1	...	1	1	1

1. **Choose** a subset of cellular automata rules (ψ_s) at random.
2. **Evaluate** the fitness of each rule.
3. **Select** three best-performing rules.
4. **Copy** the best-performing rules to the lesser-performing rules.
5. **Mutate** the lesser-performing rules.
6. **Go to Step 2** unless the stopping criteria are satisfied.

Fig. 9. Evolutionary learning of cellular automata rules.

tion, we used five-neighbor (i.e., “above”, “below”, “left”, “right”, and itself) cellular automata with values 0 and 1. The next state of a site at location (i, j) depended on its present state and the states of its four neighbors at locations $(i - 1, j)$, $(i + 1, j)$, $(i, j - 1)$, and $(i, j + 1)$. The rule of state transition ψ was denoted by

$$S_{i,j}(t + 1) = \psi[S_{i-1,j}(t), S_{i+1,j}(t), S_{i,j-1}(t), S_{i,j+1}(t), S_{i,j}(t)] \tag{1}$$

Without any doubt, the chances of finding more appropriate FDs would be higher if a large number of neighbors (e.g., eight neighbors) were considered for each state transition used. But, in the meantime, the number of rules grew combinatorial. In contrast, too small a number of neighbors (e.g., only two neighbors) would not be sufficient to provide an appropriate search of FDs. The number that we chose (i.e., 4) was a compromise. We noted that the rule set was still very large even though only four neighbors were taken into account in the present implementation. The number was about 4 billion (i.e., 4,294,967,296), as shown in Table 2. In this study, evolutionary learning algorithm was applied to select an appropriate subset of rules. They were selected at random initially and varied through evolutionary learning (Fig. 9).

3. Application domains and experimental results

The first experiment was to test the differentiation capability of this system. Then, we examined whether there

existed some common patterns among cancerous cells. In addition to the above domain, the system was also applied to two other problem domains. One was to differentiate two different types of maple leaves, which had similar morphological contours. The other domain was to separate water lilies from maple leaves, parts of which had similar morphological contours.

3.1. Cell differentiation

Our data set consisted of 80 cell patterns, each comprised of 32×32 bits. We trained this system with forty of these patterns and then tested it with the remaining 40 patterns. Ten FDs were used, each consisting of 8×8 bits. For each FD, the initial value of each bit was decided at random (i.e., either 0 or 1). Simulation was terminated after 500 cycles. At that stage, the system was able to differentiate the training set completely (note that one day was required to perform the above experiment using a Pentium-IV PC).

During the course of evolutionary learning, we kept a record of best-performing FDs for each learning cycle. Three best-performing FDs were selected, as shown in Fig. 10 (to be referred to as FD_1 , FD_2 , and FD_3 , respectively). The following was to examine how well we could use these three FDs to discriminate between cancerous cells and normal cells. Note that an FD was promising if it had a good match with at least one of these cancerous cells, and in the meantime it should not match any of nor-

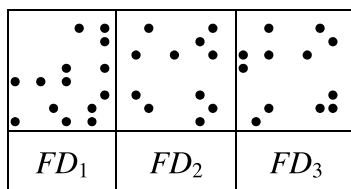


Fig. 10. Best-performing FDs.

Table 3
Test rates of each FD

	Correctly judge cancerous cells (true positive)	Misjudge normal cells as cancerous cells (false positive)
FD_1	20/20 (100%)	4/20 (20%)
FD_2	18/20 (90%)	3/20 (15%)
FD_3	17/20 (85%)	5/20 (25%)

Table 4
Number of FDs that could be used to identify each cancerous cell

Cell pattern	A	B	C	D	E	F	G	H	I	J	K	L	M	N	O	P	Q	R	S	T
Number of FDs	2	3	3	1	2	3	3	1	1	3	3	2	3	3	3	2	3	3	3	3

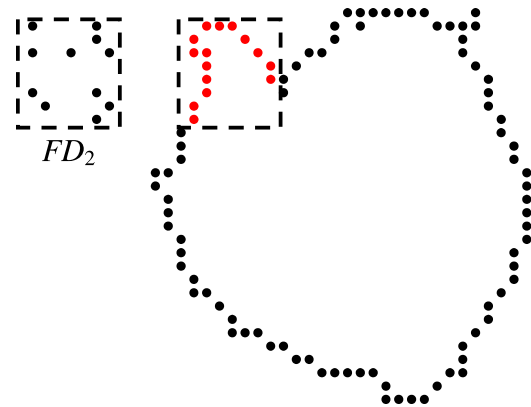


Fig. 11. Portion of a cancerous cell that FD_2 matched.

mal cells. As mentioned above, the test set consisted of 40 patterns. One half of these patterns were normal cells and the other half was of cancerous cells (see Appendix A). We tested every cell pattern with each of these three FDs in sequence.

The experimental result showed that FD_1 could successfully identify each of these twenty cancerous cell patterns. That is, it did not misjudge a cancerous cell as a normal cell. The existence of such an FD indicated that there existed a common pattern among these cancerous cells. As to normal cells, sixteen out of these 20 patterns did not match FD_1 . In other words, FD_1 did correctly identify most of them as normal cells. And only four out of these 20 patterns were mistaken for cancerous cells (false positive). We performed the same experiments for the other two FDs (FD_2 and FD_3). As shown in Table 3, FD_2 and FD_3 could successfully identify 18 and 17 out of these 20 cancerous cells, respectively. That is, only two and three out of these 20 cells were misjudged as normal cells. As to normal cells, three and five out of these twenty were misjudged as cancerous cells when we used FD_2 and FD_3 to test them, respectively.

Table 4 shows the number of these three FDs that we could use to identify each of these cancerous cells. Notice that, except patterns D, H, and I, there were more than one FD that could be used to detect a cancerous cell pattern. This suggested that there was more than one portion of a pattern that we could use to identify a cancerous cell. We further looked into the portion of a cell pattern that each FD matched (i.e., the portion identified as a cancerous cell). Fig. 11 shows such an example. The result showed

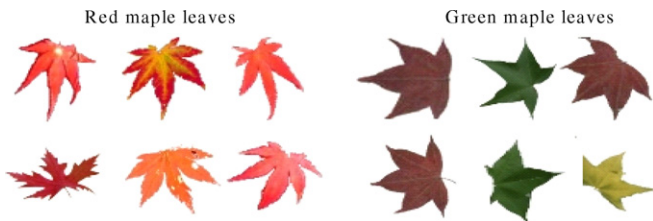


Fig. 12. Red and green maple leaves.



Fig. 14. Maple leaves and water lilies.

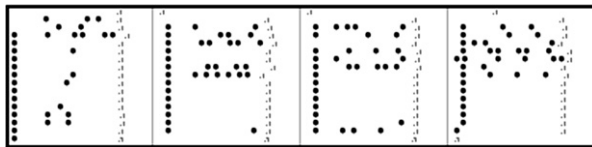


Fig. 13. Four best-performing FDs.

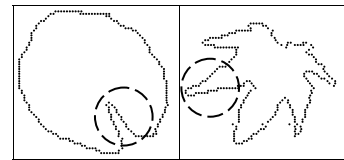


Fig. 15. An example of similar partial contours between a water lily and a maple leaf.

Table 5
Number of FDs that served to identify each pattern

Pattern	A	B	C	D	E	F	G	H	I	J
Number of FDs	4	3	4	4	4	2	4	4	3	4

that different FDs detected different portions of a pattern (see Appendix B).

3.2. Other application domains

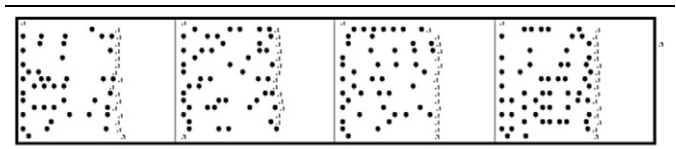
3.2.1. Red and green maple leaves

Our goal in this experiment was to test the system’s capability in differentiating similar patterns. Maple (*Acer Palmatum*) was one of the trees with leaves shaped like an open palm. Different types of maples might possess different shapes of leaves. Fig. 12 shows two of these types. Their leaves looked similar but still had slight difference. Roughly speaking, the leaves on the left of the figure (red maple leaves) were comparatively thinner, but longer, than those on the right (green maple leaves).

Twenty maple leaves were used, of which one half was green and the other half red. Each leaf pattern consisted of 64×64 bits. Ten FDs were used, each consisting of 16×16 bits. The task was to evolve these FDs so that they could separate red maple leaves from green maple leaves. Simulation was terminated when the system was able to differentiate these two types of leaves correctly. As mentioned above, the system’s performance improved continuously when the simulation proceeded. Four best-performing FDs were selected (Fig. 13).

Then, we tested the performance of each of these FDs. The test set consisted of another 20 maple leaves, of which one half was green and the other half red. Each of these

Table 6
Four best-performing FDs



four FDs was able to correctly identify at least nine out of these 10 red maple leaves. In the meantime, they successfully identified each of these 10 green maple leaves. The system achieved a higher correct classification rate (i.e., more than 90%). Table 5 shows the number of FDs that served to identify each pattern, indicating that there existed several feature patterns for separating these two types of leaves. It also showed that each FD was general (not a specific feature detector) that could be used to detect several patterns.

3.2.2. Maple and water lily

The following experiment was to separate maple leaves from water lilies. The former was like an open palm whereas the latter was like an egg with an opening (Fig. 14). At our first glance, it seemed like an easier task, as their morphological appearances were apparently different. Indeed, it was not easy when we tried to use FDs to separate them, as parts of their contours were quite similar, as shown in Fig. 15.

Our training set consisted of 20 maple leaves and 20 water lilies. Each of these patterns consisted of 64×64 bits. Simulation was terminated when the system was able to differentiate these two types of leaves correctly. Four best-performing FDs were selected (Table 6). As above, we tested each of these FDs. The test set consisted of

another 20 maple leaves and 16 water lilies. Note that this system achieved an acceptable classification rate of maple leaves (more than 85%), whereas it did pretty well in identifying each of these 20 water lilies.

4. Conclusions

Cell deformity (irregular shape), including nuclear deformity, has been one of the major methods used by pathologists to decide whether a cell is cancerous or not. Little is known about the patterns of cell deformity that can provide a definitive answer in diagnosing cancerous cells. And yet, in some cases, a normal cell may also exhibit some extents of cell deformity for some known or unknown reasons.

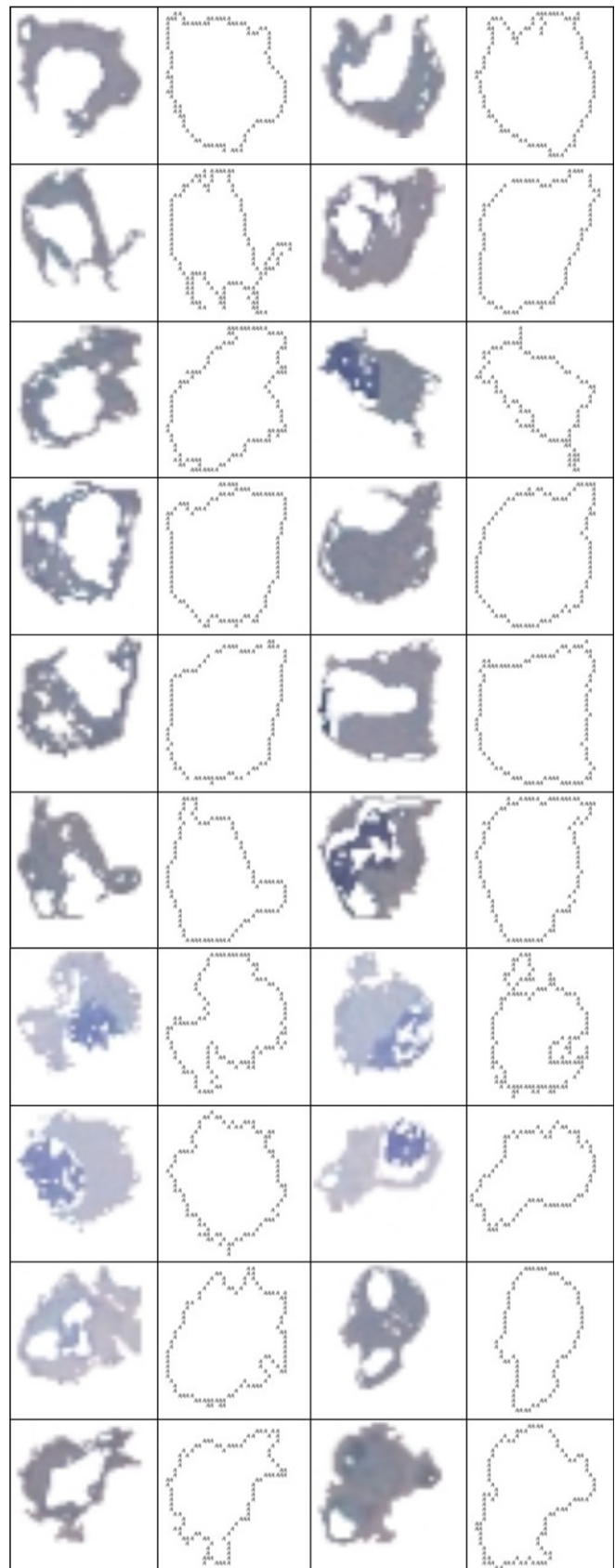
In this study, we constructed a system that was able to search for some basic feature detectors (through self-organizing learning) for separating cancerous cells from normal cells. The search was implemented by a combination of evolutionary learning algorithm and cellular automata. Our experimental result showed that this system demonstrated a high differentiation capability in separating these two types of cells. It also showed that there existed some common patterns among these cancerous cells, implying that cells with specific patterns of deformity were tentative to be cancerous. In most cases, there were two or more different patterns of deformity found within a cell. This allowed us to cross-validate a cancerous cell. Moreover, these feature detectors were general so that each of these could be used to detect a number of cancerous cells.

Different training sets might possess different feature detectors. The significance of each detector was strictly dependent upon the pattern structure of that training set. This system was also applied to two other problem domains. The experimental result showed that this system was capable of finding appropriate feature detectors for different training sets in a self-organizing manner.

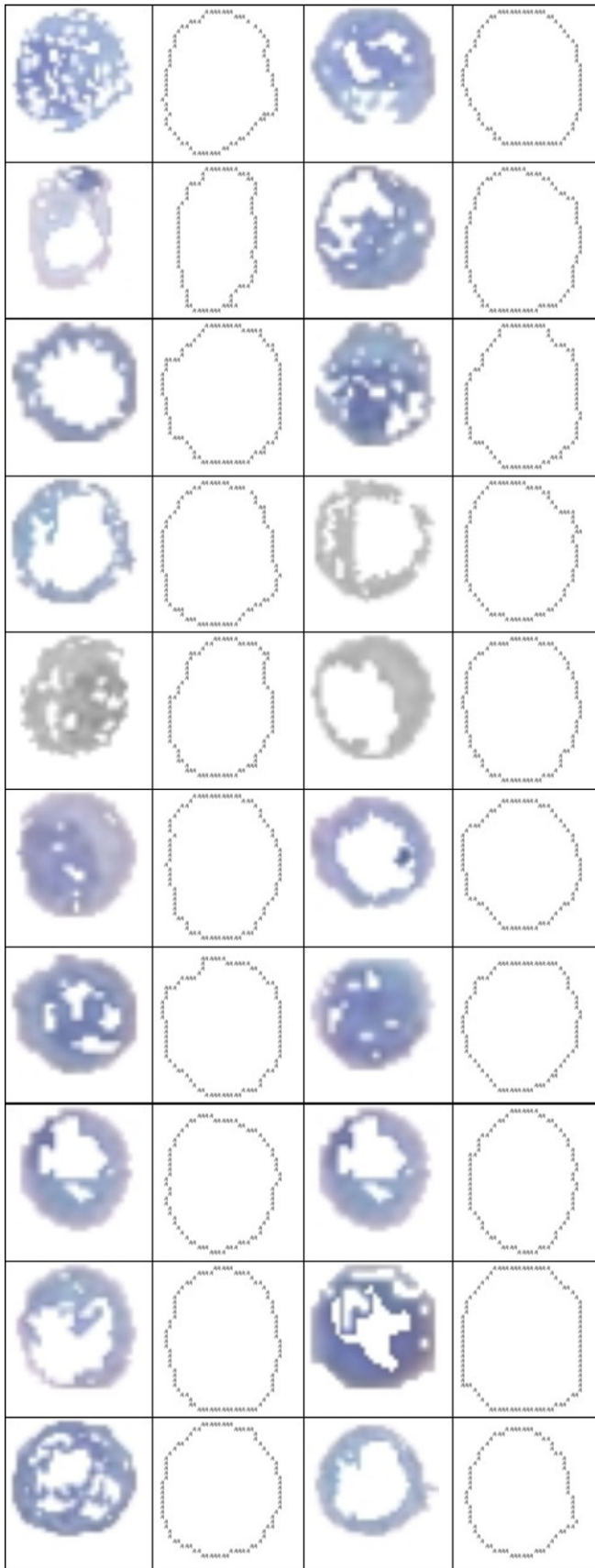
The above result has implications for both clinical studies and computational intelligence. This system can be used as an additional tool to pathologists in making medical judgments about cancerous cells. In addition, it may provide information about what patterns of cell deformity are more likely to be cancerous. This information is important as it may also help people understand the development and formation of cancerous tissues. More importantly, the ability to search for feature detectors in a self-organizing manner opens up a possibility of exploring some known or unknown patterns of cell deformity in cancerous cells. This feature is significant for computational intelligence. By altering its input–output interfaces, the model may be applied to a number of other problem domains. Future work with this model may help us indicate its power as an analytical tool.

Appendix A

Cancerous cells

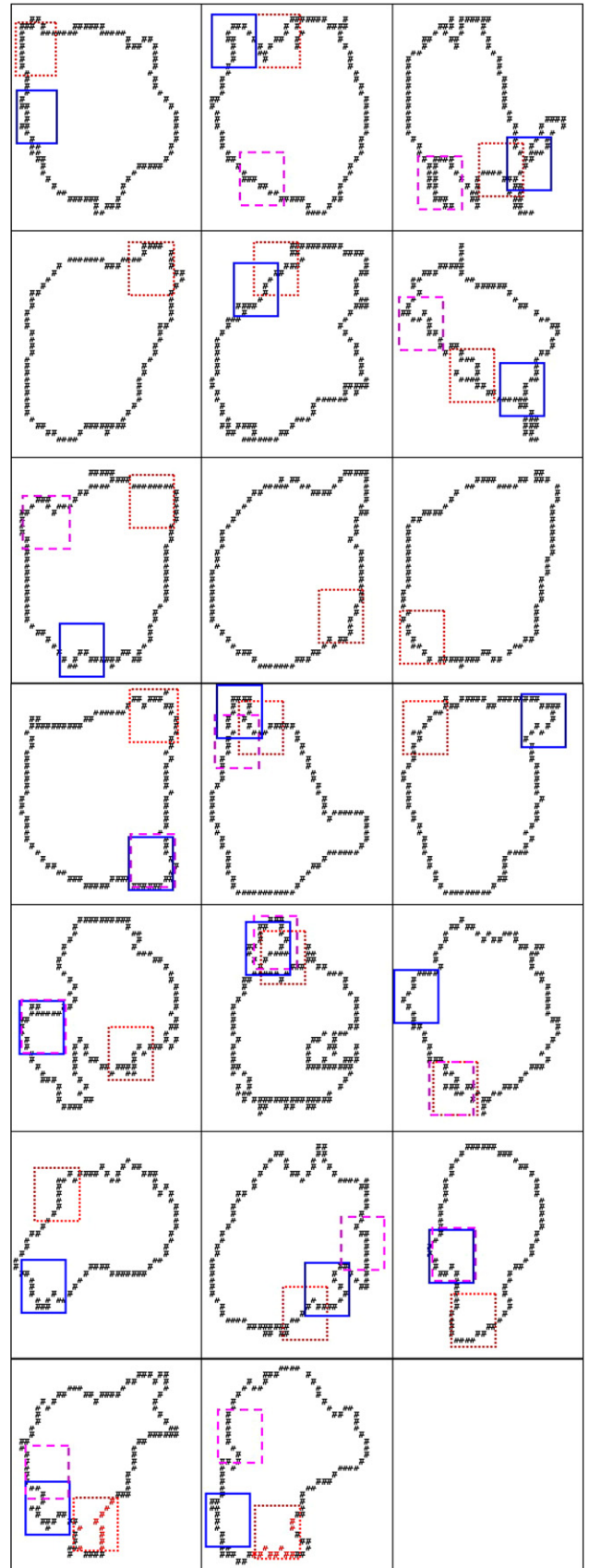


Normal cells



Appendix B

Different types of squares represent different FDs



References

- Anoraganingrum, D. (1999). Cell segmentation with median filter and mathematical morphology operation. In *Proceedings of the 10th international conference on image analysis and processing* (pp. 1043–1046).
- Bisconte, J. C., & Margules, S. (1980). Real-time continuous quantitative analysis of cultured living cells. *Mikroskopie*, 37, 204–208.
- Bremermann, H. J. (1962). Optimization through evolution and recombination. In Yovits, Jacobi, & Goldstein (Eds.), *Self-organizing systems* (pp. 93–106). Washington, DC: Springer.
- Chen, F., Xie, J., Zhang, H. & Xia, D. (2001). A technique based on wavelet and morphology transform to recognize the cancer cell in pleural effusion. In *Proceedings of the international workshop on medical imaging and augmented reality* (pp. 199–203).
- Conrad, M. (1974). Evolutionary learning circuits. *J. Theor. Biol.*, 46, 167–188.
- Fogel, D. B. (1995). *Evolutionary computation: towards a new philosophy of machine intelligence*. Piscataway, NJ: IEEE Press.
- Fogel, L. J., Owens, A. J., & Walsh, M. J. (1966). *Artificial intelligence through simulated evolution*. New York: Wiley.
- Garbay, C., Chassery, J. M., & Brugal, G. (1986). An interactive region-growing process for cell image segmentation based on local color similarity and global shape criteria. *Analytical and Quantitative Cytology and Histology*, 8, 25–34.
- Gauvain, C., Seigneurin, D., & Brugal, G. (1987). A quantitative analysis of the human bone marrow erythroblastic cell lineage using the SAMBA 200 cell image processor. *Analytical and Quantitative Cytology and Histology*, 9, 253–262.
- Hu, Y., Ashenayi, K., Veltri, R., O'Dowd, G., Miller, G., Hurst, R. & Bonner, B. (1994). A comparison of neural network and fuzzy c-means methods in bladder cancer cell classification. In *Proceedings of the IEEE international conference on neural networks* (pp. 3461–3466).
- Kim, K.-B. (1999). A physiological neuro fuzzy learning algorithm for medical image recognition. *IEEE International Fuzzy Systems*, 3(1), 140–144.
- Leung, C. C., Chan, F. H. Y., Lam, K. Y., Kwok, P. C. K. & Chen, W. F. (2000). Thyroid cancer cells boundary location by a fuzzy edge detection method. In *Proceedings of the 15th international conference on pattern recognition* (Vol. 4, pp. 4360–4363).
- Liu, Y., Zhao, T. & Zhang, J. (2002). Learning multispectral texture features for cervical cancer detection. In *Proceedings of the 2002 IEEE international symposium on biomedical imaging: macro to nano* (pp. 169–172).
- Moallemi, C. (1991). Classifying cells for cancer diagnosis using neural networks. *IEEE Expert*, 6(6), 8–12.
- Naguib, R. N. G., Sakim, H. A. M., Lakshmi, M. S., Wadehra, V., Lennard, T. W. J., Bhatavdekar, J., et al. (1999). DNA ploidy and cell cycle distribution of breast cancer aspirate cells measured by image cytometry and analyzed by artificial neural networks for their prognostic significance. *IEEE Transactions on Information Technology in Biomedicine*, 3(1), 61–69.
- Rechenberg, I. (1973). *Evolutionstrategie: Optimierung Technischer Systeme nach Prinzipien der Biologischen Evolution*. Stuttgart: Frommann-Holzboog Verlag.
- Schnorrenberg, F., Pattichis, C. S., Kyriacou, K. C., & Schizas, C. N. (1997). Computer-aided detection of breast cancer nuclei. *IEEE Transactions on Information Technology in Biomedicine*, 1(2), 128–140.
- Schnorrenberg, F., Tsapatsoulis, N., Pattichis, C. S., Schizas, C. N., Kollias, S., Vassiliou, M., et al. (2000). Improved detection of breast cancer nuclei using modular neural networks. *IEEE Engineering in Medicine and Biology*, 48–63.
- Thiran, J.-P., & Macq, B. (1996). Morphological feature extraction for the classification of digital images of cancerous tissues. *IEEE Transactions on Biomedical Engineering*, 43(10), 1011–1020.
- Travo, P., Bodin, P., Burnstock, G., & Stoclet, J. C. (1987). Quantitative method for study of morphological changes induced by vasoactive agents in single aortic myocytes grown in primary cultures. *Laboratory Investigation*, 56, 335–343.
- Wang, H., Zeng, S., Yu, C., Wang, X. & Xia, D. (2001). The researches of microscopic image segmentation and recognition on the cancer cells fallen into peritoneal effusion. In *Proceedings of the international workshop on medical imaging and augmented reality* (pp. 253–258).
- Wu, H.-S., Barba, J., & Gil, J. (1996). Region growing segmentation of textured cell images. *Electronics Letters*, 32(12), 1084–1085.